

# Diagnosis of Behavioral-Addicted Children using Electroencephalogram Dynamical Measures

Atefeh GOSHVARPOUR<sup>1</sup> and Ateke GOSHVARPOUR<sup>2,3,\*</sup>

<sup>1</sup> Department of Biomedical Engineering, Faculty of Electrical Engineering, Sahand University of Technology, Tabriz, Iran.

<sup>2</sup> Department of Biomedical Engineering, Imam Reza International University, Mashhad, Razavi Khorasan, Iran.

<sup>3</sup> Health Technology Research Center, Imam Reza International University, Mashhad, Razavi Khorasan, Iran.

E-mails: af\_goshvarpour@sut.ac.ir; ateke.goshvarpour@gmail.com;  
ak\_goshvarpour@imamreza.ac.ir

\* Author to whom correspondence should be addressed; Tel.: +98 5138041 (Ext. 3131)

Received: August 4, 2022/Accepted: September 14, 2022/ Published online: (September 25, 2022)

## Abstract

*Purpose:* The tendency to overuse the Internet is increasing with the advancement of digital technology. On the other hand, due to the availability of pornographic sites and their low protection against immature entry, children are more prone to porn addiction. Generally, diagnosing a child's addictive behavior, like pornography addiction, is made by a questionnaire, the accuracy of which is discussed by the scientific community. Consequently, the development of an automated system with electroencephalogram (EEG) signal analysis has been considered recently by researchers. We envisioned evaluating either signal dynamics and performing some executive functions on diagnosis rates. *Methods:* Some geometrical indices of EEG phase space were extracted for healthy and addicted children under different conditions, including closed eyes, memorizing, executive tasks, and recalling. Different machine learning algorithms were applied to evaluate their performances in a porn-addiction recognition problem. The proposed scheme was assessed using available Mendeley Data of 14 participants (seven porn-addicted and seven healthy) at ages 13 to 15. *Results:* The results revealed a noticeable increase in the features in most brain areas of porn addicts during recall. It also highlighted the role of task dependency, classification parameter settings, and k adjustment for K-fold cross-validation on porn detection rates. Totally, performing tasks, especially memorizing and recalling, compared to resting conditions could better highlight the difference in brain dynamics between the healthy and addicted groups. *Conclusions:* The EEG dynamical features were classified with the highest accuracy of 100%, which designated the scheme as a promising computer-aided diagnosis tool for porn addiction.

**Keywords:** Addiction; Children; Phase space; Dynamics; Electroencephalography (EEG); Detection

## Introduction

The term "addiction" is used to describe the problematic excessive use of a substance such as opioids, psychedelics, alcohol, and cocaine [1]. However, this attitude has changed. Behaviors that frequently fortify reward, motivation, and the memory circuitry are now considered part of addiction

[2-4]. Examples of such behaviors include gaming, shopping, plastic surgery, sex, kleptomania, binge eating, uncontrolled gambling, Internet use, and the like [5].

With the growth of technology, the use of the Internet in everyday life has become irreplaceable. Online banking, shopping, educating, working, and gaming are just a few examples of our daily routines. On the other hand, thanks to the development of personal mobile phones, digital technologies, and social networks, there is a growing tendency for Internet communication. In the meantime, some people report signs of disorganization/dependence on excessive Internet use and complain about the consequences in their lifetime [6]. Pathological [7], problematic [8], and addictive [9,10] Internet use are terms used by scientists to describe this situation.

One specific Internet addiction is pornography addiction which may ground online erotic compulsiveness. Pornography usage increases with age and gender-dependent, mostly in men, beginning stages of development. In children aged 10–11 years, the prevalence rate is about 0.01 [11]. In contrast, its rate increases to about 0.08 in girls and 0.4 in boys aged 16–17 years [11]. However, the pornography consumption rate in children and adolescents has increased six-fold recently [12].

Early-onset pornography addiction in childhood can affect his/her behavior at an older age in diverse ways. Impulsiveness, self-control problems, shifting attention, learning disability, sleep deficiency, deprived decision-making, forgetting responsibilities, and emotion regulation deficiency are some cases in point of porn addiction consequences [13-16].

Psychologists or parents generally identify porn addictive children through observations of psychological manifestations of addiction [17,18], while the child's personal experience is disregarded. Kang et al. [19] showed that EEG signals have the potential to identify pornography addiction among children.

Previously, some studies have been conducted to evaluate the effect of Internet addiction using brain signals [20,21]. Their findings emphasized ample Internet usage influences cerebral data coding and amalgamation [20]. Additionally, changes in the EEG frequency powers can be counted as Internet addiction biomarkers [21]. Neuroscientific literature confirmed that underlying neural processes of Internet addiction are comparable to substance addiction [22]. In contrast, the EEG experiment specifically focused on pornography is in its infancy.

Voon et al. [23] evaluated persons with and without compulsive sexual behaviors to study their neural associates with sexual cue reactivity. The functional magnetic resonance imaging of 19 problematic and 19 healthy volunteers was considered while watching sexually explicit/nonsexual exciting videos. Sexual clips caused more engagement of limbic circuits of the corticostriatal in addicts, which was characterized by the activation of some brain regions like the amygdala, ventral striatum, and the dorsal anterior cingulate.

Prause et al. [24] assessed evoked potentials of hypersexual behavior (excessive viewing of visual sexual stimuli) of addictive persons. Explicit sexual images were shown for 122 participants (36 women and 86 men) who reported or denied addictive visual sexual stimuli use. Simultaneously, the evoked response potentials were recorded. The results revealed that modulation of the badly hypersexual behaved group and the desired level for sex with a partner predicted late positive potentials amplitude. Those who reported problems regulating visual sexual stimuli use and higher libido had lower late positive potentials responses to visual sexual stimuli.

Kamaruddin et al. [25] assessed the EEG of the frontal region during eye-open and eye-close resting states of addicted and non-addicted participants. Analyzing EEG frequency bands revealed lower-alpha wave activity in the frontal brain region of addicted compared to non-addicted participants. Kamaruddin et al. [26] extracted in 2019 the Mel Frequency Cepstral Coefficient (MFCC) of EEG bands and fed the indices to some classifiers, including Random Forest (RF), Naive Bayesian (NB), and Multi-Layer Perceptron (MLP). The experimental results revealed that the MLP classifier outperformed the other classifiers, resulting in a maximum accuracy of 89%.

Xiaoxi et al. [27] studied the frontal EEG, including F3, F4, F7, F8, Fp1, Fp2, and Fz electrodes of 7 porn addicts and 7 healthy participants in the age range of 13 to 15 years. Utilizing wavelet analysis and support vector machine (SVM), a maximum accuracy of 81.71% was reported for porn addiction recognition.

The shortcomings of previous literature in assessing brain dynamics in porn-addicted people prompted us to address this issue. The current study evaluated EEG signals of teenagers with and

without porn addiction using phase space-based measures during the performance of different tasks. Several classifiers were applied to appraise the scheme efficiency in a porn-addicted EEG classification problem.

### Material and Method

Figure 1 shows the flowchart of the proposed algorithm. Its components are described in the following sub-sections.

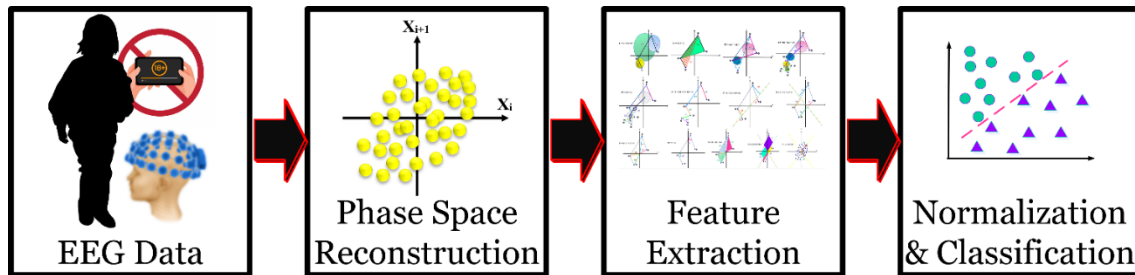


Figure 1. The proposed algorithm

#### Electroencephalogram Data

Available “Mendeley Data” [28] was studied in the current experiment, while detailed information on the dataset is accessible in Xiaoxi et al. [29].

The electroencephalogram (EEG) signals of 14 participants were recorded. Five girls and nine boys in the age range of 13 to 15 years participated in the study [29]. A psychologist’s clinical evaluation confirmed the seven porn-addicted and the seven healthy young people. To this effect, a primary screening tool was used which was available online and free of charge. It is for teenagers aged 12 to 18 and is called “Youth Pornography Addiction Screening Tool (YPAST)” [30,31].

The signals were collected using a 19-channel Brain Maker EEG machine and digitized at the rate of 250 Hz. The EEG electrodes were placed according to the international 10-20 system, including P4, O2, P8, T8, C4, Cz, Fz, F4, Fp2, F8, Fp1, F7, F3, C3, T7, P7, P3, O1, and Pz. A 10-minute protocol was designed. The participants had the following nine different tasks:

- (1) One-second closed-eyes (EC).
- (2) One-minute open-eyes (EO)
- (3) One-minute happy pictorial stimulation (H)
- (4) One-minute calm inducement (C)
- (5) One-minute sad incentive (S)
- (6) One-minute fearful stimulus (F)
- (7) One-minute 15 words memorizing (M)
- (8) Two-minute executive task (ET)
- (9) One-minute 15 words recalling (R).

For tasks (3) to (6), colored pictures from the International Affective Picture System (IAPS) [32] were shown on the screen to elicit a target emotion in the participants. In task M, watching individually 15 words presented on the monitor, the contributor was instructed to remember all words. In the ET, a series of pornography pictures, validated by a psychologist, was shown. In the R, the participants should spell the 15 words given in the M task, watching a white blank screen. In the current study, we used EEG signals for EC, ET, M, and R tasks.

#### Phase Space Reconstruction

The conventional phase space was reconstructed by plotting each EEG sample against the subsequent one ( $X_i, X_{i+1}$ ), where X stands for an EEG signal length of N, and  $X_i$  represents every EEG sample (for  $i \in 1, 2, \dots, N-1$ ).

Feature Extraction

To quantify the phase space trajectory, 13 features (F) were used, as described in Table 1. The used features are as follows:

$$F1 = \sum_{i=1}^{N-2} \frac{\pi}{4} ((X_{i+1} - X_i)^2 + (X_{i+2} - X_{i+1})^2) \tag{F1}$$

$$F2 = \frac{1}{2} \sum_{i=1}^{N-3} \left| \det \begin{bmatrix} X_i & X_{i+1} & X_{i+2} \\ X_{i+1} & X_{i+2} & X_{i+3} \\ 1 & 1 & 1 \end{bmatrix} \right| \tag{F2}$$

$$F3 = \pi \sum_{i=1}^{N-3} \left( \frac{\det \begin{bmatrix} X_i & X_{i+1} & X_{i+2} \\ X_{i+1} & X_{i+2} & X_{i+3} \\ 1 & 1 & 1 \end{bmatrix}}{A} \right)^2, \tag{F3}$$

where  $A = \sqrt{(X_{i+1} - X_i)^2 + (X_{i+2} - X_{i+1})^2} + \sqrt{(X_{i+2} - X_i)^2 + (X_{i+3} - X_{i+1})^2} + \sqrt{(X_{i+2} - X_{i+1})^2 + (X_{i+3} - X_{i+2})^2}$

$$F4 = \sum_{i=1}^{N-4} \sqrt{\left( \frac{X_{i+1} + X_{i+2} + X_{i+3}}{3} - \frac{X_i + X_{i+1} + X_{i+2}}{3} \right)^2 + \left( \frac{X_{i+2} + X_{i+3} + X_{i+4}}{3} - \frac{X_{i+1} + X_{i+2} + X_{i+3}}{3} \right)^2} \tag{F4}$$

$$F5 = \sum_{i=1}^{N-5} \frac{(X_{C_{i+1}} - X_{C_i})(X_{C_{i+2}} - X_{C_{i+1}}) + (Y_{C_{i+1}} - Y_{C_i})(Y_{C_{i+2}} - Y_{C_{i+1}})}{\sqrt{(X_{C_{i+1}} - X_{C_i})^2 + (Y_{C_{i+1}} - Y_{C_i})^2} + \sqrt{(X_{C_{i+2}} - X_{C_{i+1}})^2 + (Y_{C_{i+2}} - Y_{C_{i+1}})^2}} \tag{F5}$$

where  $(X_{C_i}, Y_{C_i})$  is the coordinate of the Heron's circular center.

$$F6 = \sum_{i=1}^{N-2} \sqrt{(X_{i+1} - X_i)^2 + (X_{i+2} - X_{i+1})^2} \tag{F6}$$

$$F7 = \sum_{i=1}^{N-1} \frac{|X_{i+1} - X_i|}{\sqrt{2}} \tag{F7}$$

$$F8 = \sum_{i=1}^{N-1} \frac{|X_{i+1} + X_i|}{\sqrt{2}} \tag{F8}$$

$$F9 = \sum_{i=1}^{N-1} \sqrt{X_i^2 + X_{i+1}^2} \tag{F9}$$

$$F10 = \sum_{i=1}^{N-3} \frac{(X_{i+1} - X_i)(X_{i+2} - X_{i+1}) + (X_{i+2} - X_{i+1})(X_{i+3} - X_{i+2})}{\sqrt{(X_{i+1} - X_i)^2 + (X_{i+2} - X_{i+1})^2} + \sqrt{(X_{i+2} - X_{i+1})^2 + (X_{i+3} - X_{i+2})^2}} \tag{F10}$$

$$F11 = \frac{1}{2} \sum_{i=1}^{N-2} \left| \det \begin{bmatrix} 0 & X_i & X_{i+1} \\ 0 & X_{i+1} & X_{i+2} \\ 1 & 1 & 1 \end{bmatrix} \right| \tag{F11}$$

$$F12 = \sum_{i=1}^{N-1} \frac{|X_{i+1} + X_i| |X_{i+1} - X_i|}{2} \tag{F12}$$

$$F13 = \pi \times SD1 \times SD2 \tag{F13}$$

Table 1. Description of the features

Feature	Description
F1	Suppose each pair of points of the phase space $((X_i, X_{i+1}), (X_{i+1}, X_{i+2}))$ as the diameter of a circle. The area of each circle is calculated. Then, the F1 is intended by the summation of all circles area [33]. Considering $C_i$ as a circles area, an illustration of F1 calculation is shown in Figure 2(a).
F2	Suppose three corners of a triangle that formed by every triple subsequent point of the phase space $((X_i, X_{i+1}), (X_{i+1}, X_{i+2}), (X_{i+2}, X_{i+3}))$ . The area of each triangle is calculated. Next, the F2 is achieves by the summation of successive triangles area [34]. Considering $T_i$ as a triangle area, an illustration of F2 calculation is presented in Figure 2(b).
F3	Alike to F2, a triangle is formed. Then, a circle within each triangle is drawn with radius $r_i$ , known as Heron's circular area $(\pi r_i)$ . The summation of Heron's circular areas is the F3 [35]. Figure 2(c) illustrates an example of F3 calculation.
F4	Similar to the F3, a Heron's circle is formed. Then, the centroid of each Heron's circle was obtained. Finally, the summation of the distance $(D_i)$ between every two centroid circles is calculated [34]. Figure 2(d) exemplifies the F4 calculation.
F5	Consider the centers of three consecutive Heron's circle. The F5 is defined as the summation of the angle $(\theta_i)$ between each three centroid circles [34]. Figure 2(e) typifies the F5 calculation.
F6	It is defined as the summation of successive vector lengths $(L_i)$ of each successive pair of points [36]. Figure 2(f) represents the F6 calculation.
F7	Forming the identity line (i.e. $y = x$ ), the width of the phase space from this line is measured. The F7 is designated as the summation of the shortest distance $(S_i)$ from each point in proportion to the 45-degree line [34]. Figure 2(g) symbolizes the F7 calculation.
F8	Forming the line perpendicular to the identity line (i.e. $y = -x$ ), the width of the phase space from this line is measured. The F8 is designated as the summation of the shortest distance $(V_i)$ from each point in proportion to the 135-degree line [34]. Figure 2(h) symbolizes the F8 calculation.
F9	For F9 calculation, the distance of any point on the coordinate plane to the coordinate center $(O_i)$ is considered. Then, the summation of these distances is computed, as shown in Figure 2(i) [36].
F10	To extract F10, the summation of the angles $(\alpha_i)$ between three consecutive points is measured using the following equation (Figure 2(j)) [33].
F11	Assume two consecutive points on the phase space $((X_i, X_{i+1}), (X_{i+1}, X_{i+2}))$ and the coordinate center $(0, 0)$ as the corners of a triangle. The F11 is described by the summation of the area of the triangles $(TO_i)$ obtained by these corners [34]. An example of F11 calculation is demonstrated in Figure 2(k).
F12	Consider the vertex of the coordinate plane $(0, 0)$ and a point on the phase space $(X_i, X_{i+1})$ as the two corners of a rectangle. Additionally, assume the shortest distance from that point to 45 and 135-degree lines as the two edges of the identical rectangle. The area of the formed rectangle is shown by $RA_i$ . The F12 is defined as the summation of the concessive rectangular area (Figure 2(l)) [34].
F13	Consider the identity line and the line perpendicular to it. The standard deviation of the phase space shape with respect to the former is known as SD2 $(SD2 = \sqrt{\text{variance}(X_i - X_{i+1}/\sqrt{2})})$ , and the standard deviation of the phase space shape with respect to the latter is known as SD1 $(SD1 = \sqrt{\text{variance}(X_i + X_{i+1}/\sqrt{2})})$ . F13 quantifies the scattering of data points on the phase space (Figure 2(m)) [37].

Normalization and Classification

Consider F is the feature,  $F_{\min}$  and  $F_{\max}$  are the minimum and the maximum values of the feature. The extracted features were normalized (NF) in the range of -1 to 1 as shown in Eq. (1):

$$NF = 2\left(\frac{F - F_{\min}}{F_{\max} - F_{\min}}\right) - 1 \tag{1}$$

After normalization, the feature vector was inputted into the following classifiers.

- 1- Naïve Bayes (NB)
- 2- Support vector machine (SVM), with a radial basis function (RBF) as a kernel.
- 3- Decision Tree (DT)

- 4- Adaboost
- 5- *K* nearest neighbor (*k*NN), with a varying value of the *k* value in the range of 1 to 20, and the Minkowski distance.

Using a *k*-fold cross-validation (CV) approach (*k* = 2 to 10), the performance of the classifiers was assessed. The *k*-fold CV is generally performed in the following steps. (1) Randomly break the full data into independent *k* segments of roughly identical size. (2) Keep one segment for the model validation and use the others for the model training. (3) Fit a classification model on the training and assess it using the validation, and calculate the model performance. (4) Repeat it *k* times to obtain *k* performance values for each repetition. (5) Calculate the average of the *k* performances.

Accuracy (AC), sensitivity (SE), specificity (SP), and F1-score (F1) criteria were calculated for evaluating the classifier performances, as follows:

$$AC (\%) = \frac{True\ Positive + True\ Negative}{True\ Positive + True\ Negative + False\ Positive + False\ Negative} \times 100 \quad (2)$$

$$SE (\%) = \frac{True\ Positive}{True\ Positive + False\ Negative} \times 100 \quad (3)$$

$$SP (\%) = \frac{True\ Negative}{True\ Negative + False\ Positive} \times 100 \quad (4)$$

$$F_1 (\%) = \frac{2 \times True\ Positive}{2 \times True\ Positive + False\ Positive + False\ Negative} \times 100 \quad (5)$$

All simulations were done in MATLAB R2014a.

## Results

Figure 3 shows the variations of the extracted features in different EEG channels and different states for addicted and non-addicted participants.

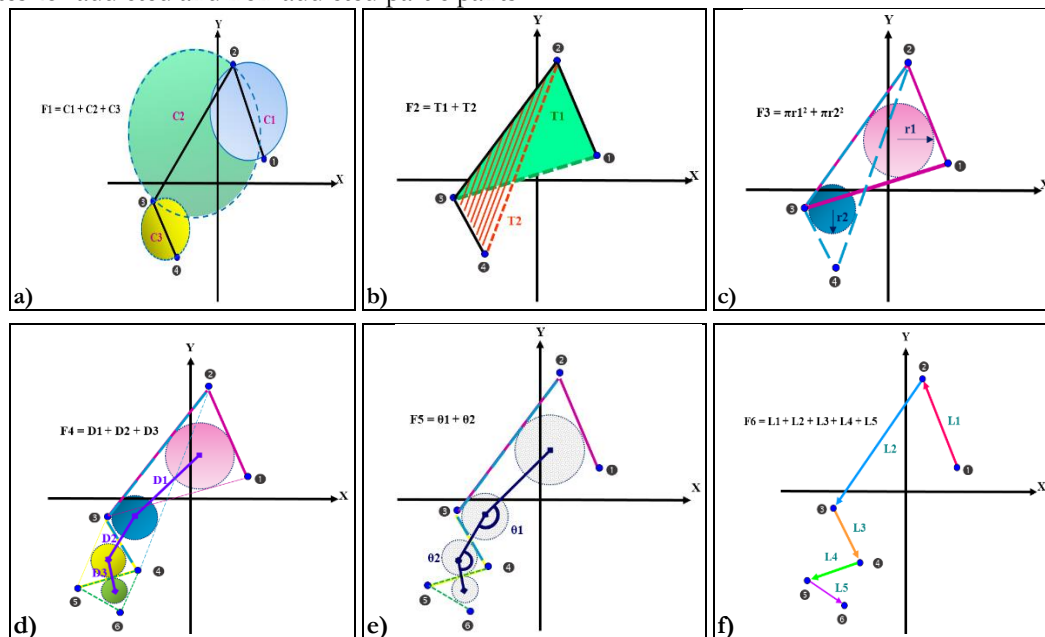


Figure 2. Illustration of the features extracted from the phase space: (a) F1, (b) F2, (c) F3, (d) F4, (e) F5, (f) F6

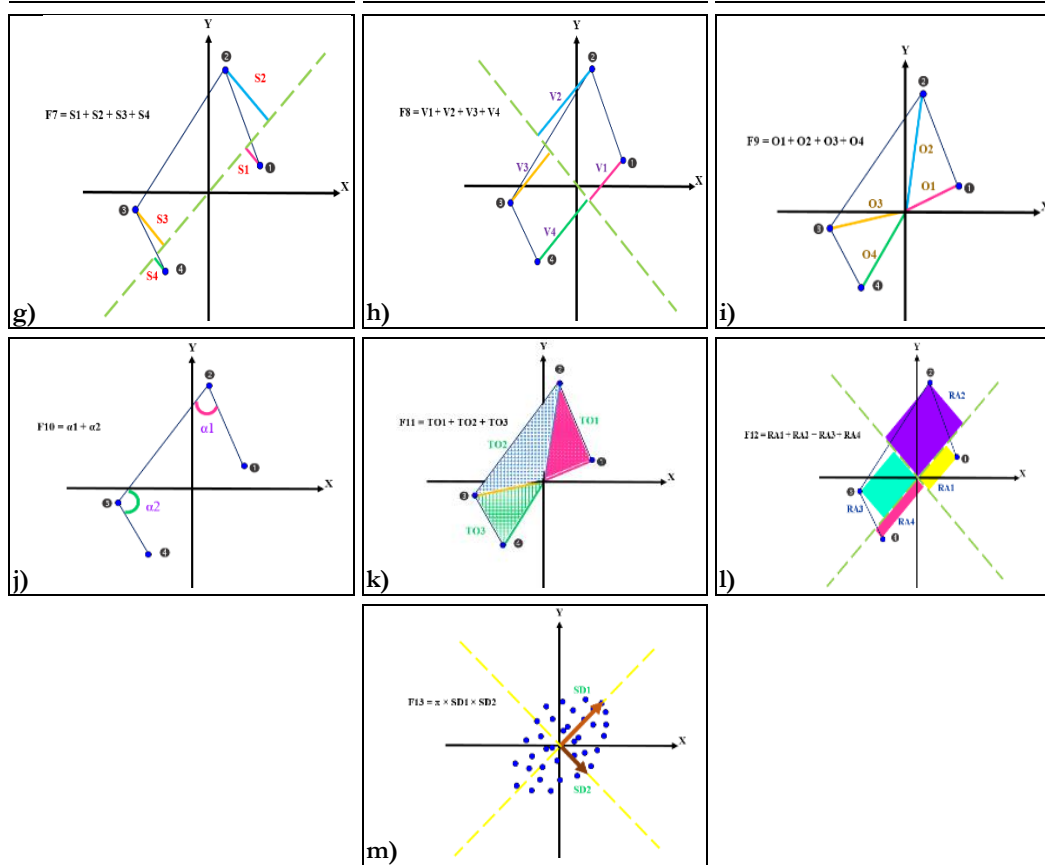


Figure 2. (continuation) Illustration of the features extracted from the phase space: (g) F7, (h) F8, (i) F9, (j) F10, (k) F11, (l) F12, (m) F13.

Figure 3 shows differences between the healthy and addicted groups for all extracted features in different brain areas, especially for R, M, and ET tasks. In particular, healthy individuals had lower brain activity in most brain areas than addicts for R. In contrast, no difference was observed between the features of the two groups for EC.

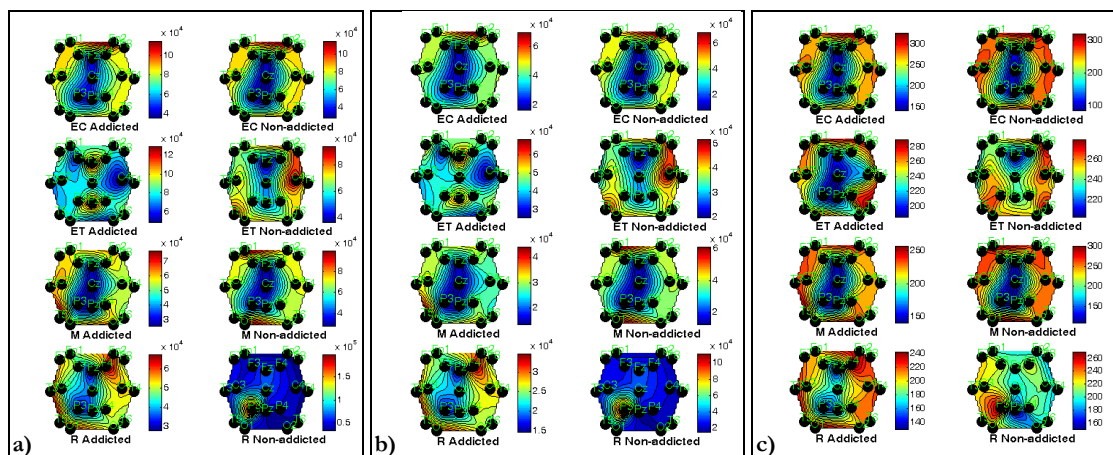
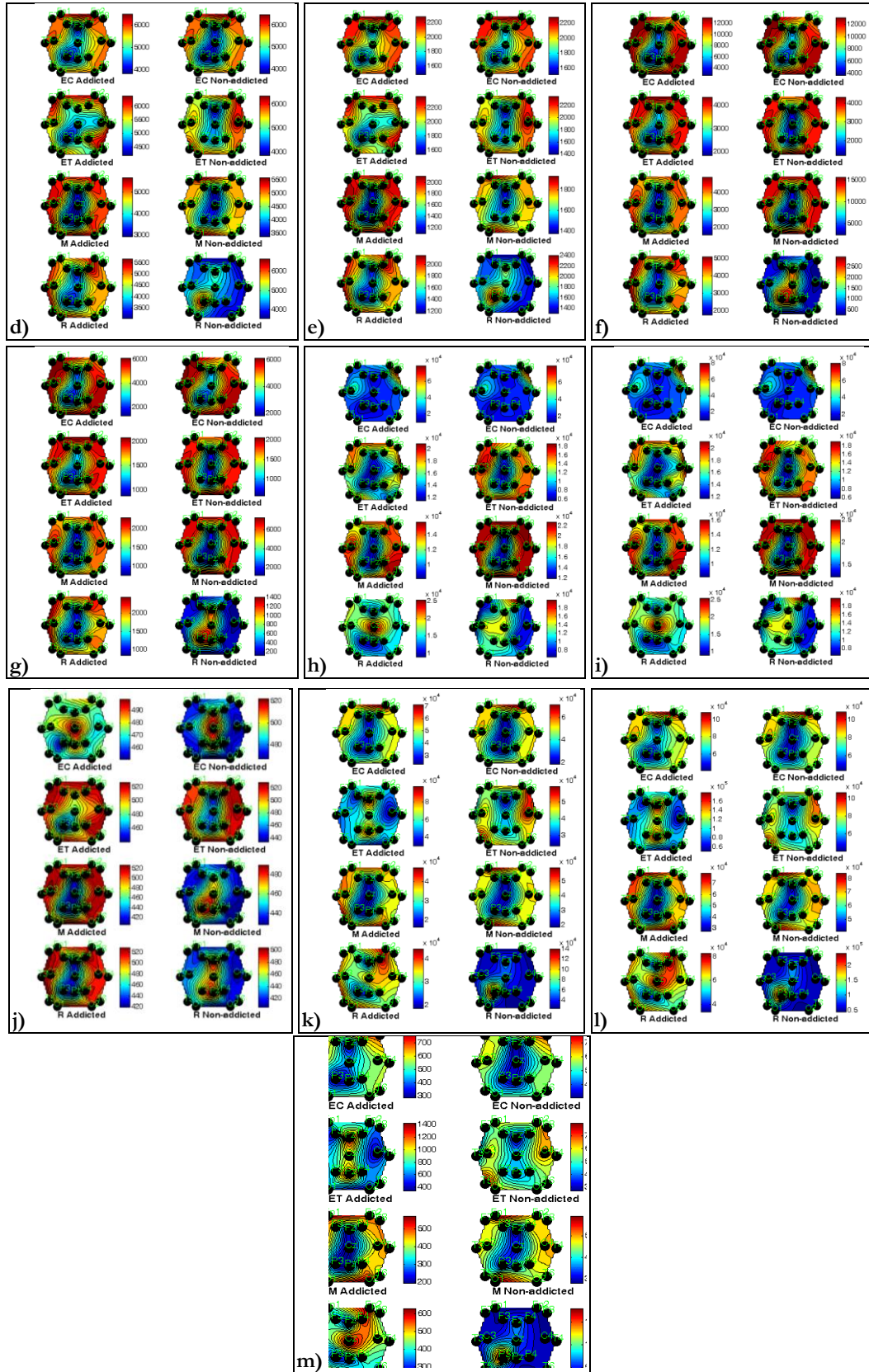


Figure 3. Variation of features over the 19-channel EEG for the 'EC', 'ET', 'M', and 'R' tasks for addicted and non-addicted groups: (a) F1, (b) F2, and (c) F3.

Table 2 abbreviates the detection rates of EC, ET, M, and R. Precisely, it shows the highest classification achievements and the corresponding k for the k-fold CV for each class.



**Figure 3.** (continuation) Variation of features over the 19-channel EEG for the ‘EC’, ‘ET’, ‘M’, and ‘R’ tasks for addicted and non-addicted groups: (d) F4, (e) F5, (f) F6, (g) F7, (h) F8, (i) F9, (j) F10, (k) F11, (l) F12, and (m) F13.

Table 2a). The highest classification results of different group and the corresponding k value for CV: a) EC

Classifier	k for CV	AC	SE	SP	F1
NB	6	88.57	100	81.82	86.67
Adaboost	8	96.15	100	100	96
3NN	6	94.29	94.29	96.43	94.29
6NN	2	98.11	96.3	100	98.11
9NN	5	97.62	95.45	100	97.67
12NN	8	100	100	100	100
15NN	4	96.15	100	100	96.3
18NN	2,3,6,10	100	100	100	100
SVM	10	100	100	100	100
1NN	6	91.43	91.84	100	92.04
4NN	4	91.43	91.43	100	91.43
7NN	9	95.24	95.24	100	95.24

Classifier	k for CV	AC	SE	SP	F1
10NN	8	97.28	100	100	94.44
13NN	7	100	100	100	100
16NN	8,100	100	100	100	100
19NN	3,5,6,8	100	100	100	100
DT	9	95.65	91.67	100	95.65
2NN	5	92.38	90.74	94.12	92.45
5NN	7	98.11	96.43	100	98.18
8NN	6	100	100	100	100
11NN	5,10	94.29	100	100	94.74
14NN	5,10	100	100	100	100
17NN	3,9	100	100	100	100
20NN	4,10	100	100	100	100

Note – CV: Cross-validation, AC: Accuracy, SE: Sensitivity, SP: Specificity, F1: F1-score, NB: Naïve Bayes, SVM: Support Vector Machine, kNN: k-nearest neighbor, ≠: All except for.

Table 2b). The highest classification results of different group and the corresponding k value for CV: b) ET

Classifier	k for CV	AC	SE	SP	F1
NB	8	84.62	100	90	83.33
Adaboost	10	100	100	100	100
3NN	10	91.43	89.19	93.94	91.67
6NN	5	94.34	96	92.86	94.12
9NN	10	88.57	92.86	100	89.47
12NN	6	96.67	100	100	96.55
15NN	4	100	100	100	100
18NN	6	95.65	91.67	100	95.65
SVM	8	96.15	100	100	96.3
1NN	2	88.57	87.27	90	88.89
4NN	6	85.71	82.14	100	87.5
7NN	8	97.62	100	95.45	97.56

Classifier	k for CV	AC	SE	SP	F1
10NN	3	94.29	94.44	94.12	94.44
13NN	3	90	100	100	90.32
16NN	3	100	100	100	100
19NN	6,10	100	100	100	100
DT	6	94.29	89.47	100	94.44
2NN	3	85.71	83.64	88	85.98
5NN	8	92.31	86.67	100	92.86
8NN	5	92.86	87.5	100	93.33
11NN	5	91.43	89.47	100	92.31
14NN	9	100	100	100	100
17NN	2	100	100	100	100
20NN	7	100	100	100	100

Note – CV: Cross-validation, AC: Accuracy, SE: Sensitivity, SP: Specificity, F1: F1-score, NB: Naïve Bayes, SVM: Support Vector Machine, kNN: k-nearest neighbor, ≠: All except for.

Table 2c). The highest classification results of different group and the corresponding k value for CV: c) M

Classifier	k for CV	AC	SE	SP	F1
NB	8	96.15	92.86	100	96.3
Adaboost	All	100	100	100	100
3NN	4-10	100	100	100	100
6NN	≠5	100	100	100	100
9NN	2,3,5,6,9,10	100	100	100	100
12NN	All	100	100	100	100
15NN	All	100	100	100	100
18NN	All	100	100	100	100
SVM	All	100	100	100	100
1NN	2,3,6	100	100	100	100
4NN	2,4	100	100	100	100
7NN	2,3,8-10	100	100	100	100

Classifier	k for CV	AC	SE	SP	F1
10NN	All	100	100	100	100
13NN	All	100	100	100	100
16NN	All	100	100	100	100
19NN	All	100	100	100	100
DT	6,8-10	100	100	100	100
2NN	2	98.1	98	100	98.15
5NN	6-10	100	100	100	100
8NN	All	100	100	100	100
11NN	All	100	100	100	100
14NN	All	100	100	100	100
17NN	All	100	100	100	100
20NN	All	100	100	100	100

Note – CV: Cross-validation, AC: Accuracy, SE: Sensitivity, SP: Specificity, F1: F1-score, NB: Naïve Bayes, SVM: Support Vector Machine, kNN: k-nearest neighbor, ≠: All except for.

**Table 2d).** The highest classification results of different group and the corresponding k value for CV: D) R

Classifier	k for CV	AC	SE	SP	F1
NB	10	81	100	76.9	77.8
Adaboost	≠2	100	100	100	100
3NN	4-8,10	100	100	100	100
6NN	≠9	100	100	100	100
9NN	≠3,7	100	100	100	100
12NN	≠2	100	100	100	100
15NN	All	100	100	100	100
18NN	All	100	100	100	100
SVM	≠2	100	100	100	100
1NN	2-5	100	100	100	100
4NN	2,3	100	100	100	100
7NN	4,8-10	100	100	100	100

Classifier	k for CV	AC	SE	SP	F1
10NN	All	100	100	100	100
13NN	All	100	100	100	100
16NN	All	100	100	100	100
19NN	All	100	100	100	100
DT	9	100	100	100	100
2NN	2	97.1	94.6	100	97.3
5NN	6-10	100	100	100	100
8NN	All	100	100	100	100
11NN	All	100	100	100	100
14NN	≠4	100	100	100	100
17NN	All	100	100	100	100
20NN	All	100	100	100	100

Note – CV: Cross-validation, AC: Accuracy, SE: Sensitivity, SP: Specificity, F1: F1-score, NB: Naïve Bayes, SVM: Support Vector Machine, kNN: k-nearest neighbor, ≠: All except for.

In brief, the results of Table 2 reveals that kNN resulted in a maximum accuracy of 100%. However, the classification rates were highly dependent on the task, classifier parameters/structures, and the number of k for CV. The highest porn-addiction recognition rates were achieved for task M, and the second-best results were devoted to task R.

### Discussions

Comparing topographic maps of EEG dynamic measures of healthy and addicted children revealed the greatest difference in task-R, which showed an increase in the value of features of most brain channels for addicts (Figure 3). The executive function generally designates a complex interaction between many cognitive domains to expedite targeted behaviors [38]. Studies have engaged the frontal lobes as the main circuits involved; however, integrating a difference between the individual facets of executive functions [39,40]. Consequently, in several previous EEG studies [16,25-29], only the brain signals of addicts in the frontal region were evaluated and other brain channels were neglected. In contrast, the results obtained in this study emphasize the importance of evaluating all EEG electrodes.

Additionally, obvious changes were produced for task-M and task-ET. This suggests that performing a task such as memorizing, recalling, and evoking emotions can clearly indicate the differences between the brain dynamics of the two groups. Although in previous studies, the brain signal of addicts usually has been analyzed in both open and closed eyes conditions in resting state [16,25,26], our study emphasizes that the brain manifestations of addicts during the tasks performances show more drastic changes than when the task was not performed.

The performance of NB, SVM, DT, Adaboost, and kNN was evaluated in the discrimination of healthy and addicted youngsters. Table 2 shows the following:

- The disability of Naïve Bayes in perfectly discriminating the groups was revealed for different tasks. For the ‘M’ task, the maximum accuracy was 96.15%. However, its porn detection rate dropped to about 80% for ‘R’.
- SVM could detect the groups of all tasks with an accuracy of 100%, except for the ‘ET’ task, where the highest recognition rate was 96.15%.
- Using DT, the classification rates fluctuated between 94.29 and 100%. A maximum recognition rate was 100% for ‘M’ and ‘R’ tasks.
- Adaboost could classify the groups successfully with a rate of 100%, except for the ‘EC’ task, where the maximum recognition rate was 96.15%.

- Depending on the task, classification parameters, and a value of k for CV, kNN produced different results. For 8NN, 12NN-14NN, and 16NN-20NN, the highest performance of 100% was achieved during 'EC'. For 'ET', porn addiction was diagnosed perfectly (with a rate of 100%) using 14NN-17NN, 19NN, and 20NN. A recognition rate of 100% was realized for 'M' and 'R' using 1NN, 3NN-20NN. However, the value of k for the CV that resulted in the highest performances was variable.
- Totally, the best porn addiction detection rates were for the 'M' task. The second best results were assigned to 'R'.

The highest detection rate of porn addicts in the Kamaruddin et al. [25] study was 89%, obtained by the MFCC coefficients of EEG frequency bands and MLP. Xiaoxi et al. [27,28,29] also reported a maximum accuracy of 81.71% using wavelet analysis and a support vector machine. As a result, the proposed algorithm has provided significant results in terms of classification performance.

The current study suffers from some restrictions, which should be inspected in the subsequent studies. First, we examined only a limited number of the signal phase space indices to evaluate the EEG dynamics. A range of nonlinear indices has been proposed that can be analyzed in future studies to more accurately assess differences in brain dynamics between addicted and healthy individuals. Second, the number of participants in the present study was limited, and we evaluated signal dynamics for some specific tasks. In future studies, more samples and more executive tasks should be appraised. Third, we did not include the effect of gender in our study, while it is an influential factor in porn addiction. In future studies, brain analyzes should be performed in a gender-dependent form. Forth, the database has not provided any information about if the case and control subjects from the database were consecutive or a random sample of patients and if the selection of those subjects avoided inappropriate exclusions. All these questions indicate a high risk of bias for patient selection that must be reported. Additionally, the test cohort's participants should ideally mirror the intended clinical population, including the distribution of the relevant clinical outcomes. The following studies should collect and analyze a richer database concerning the number of samples and the studied population.

## Conclusions

Performing tasks compared to rest with eyes closed could better demonstrate the difference in brain dynamics between the healthy and addicted groups. The uttermost difference was observed for recalling, where feature value was increased for porn addicts in most brain areas. Furthermore, task dependency, classification parameter settings, and k adjustment for K-fold CV are important detection factors. The EEG dynamical features were classified with the highest accuracy of 100%, which nominated our scheme as a promising technique for detecting porn-addicted children.

## Compliance with Ethical Standards

**Funding:** This research did not receive any specific grant from funding agencies in the public, commercial, or not-for-profit sectors.

**Conflict of Interest:** The authors declare that they have no conflict of interest.

**Statements of ethical approval:** This article does not contain any studies with human participants performed by any of the authors.

## References

1. White WL. *Slaying the Dragon: The History of Addiction Treatment and Recovery in America*, 1st ed.; Chestnut Health Systems: Bloomington, IL, USA, 1998.

2. Grant JE, Potenza MN, Weinstein A, Gorelick DA. Introduction to behavioral addictions. *Am J Drug Alcohol Abuse* 2010;36:233-241.
3. Olsen CM. Natural rewards, neuroplasticity, and non-drug addictions. *Neuropharmacology* 2011;61:1109-1122.
4. Pitchers KK, Vialou V, Nestler EJ, Laviolette SR, Lehman MN, Coolen LM. Natural and drug rewards act on common neural plasticity mechanisms with  $\Delta$ FosB as a key mediator. *J Neurosci Off J Soc Neurosci*. 2013;33:3434-3442.
5. Potenza MN. Non-substance addictive behaviors in the context of DSM-5. *Addict Behav*. 2014;39(1):1-2. doi:10.1016/j.addbeh.2013.09.004
6. Weinstein A, Lejoyeux M. Internet addiction or excessive Internet use. *Am J Drug Alcohol Abuse*. 2010;36:277-283.
7. Davis R. A cognitive-behavioral model of pathological Internet use. *Computers in Human Behavior* 2001;17:187-195.
8. Caplan SE. Problematic Internet use and psychosocial well-being: Development of a theory-based cognitive-behavioral measurement instrument. *Computers in Human Behavior* 2002;18:553-575.
9. Widyanto L, Griffiths M. "Internet addiction": A critical review. *International Journal of Mental Health and Addiction* 2006;4:31-51.
10. Young KS. Internet addiction: A new clinical phenomenon and its consequences. *American Behavioral Scientist* 2004;48:402-415.
11. Wolak J, Mitchell K, Finkelhor D. Unwanted and wanted exposure to online pornography in a national sample of youth internet users. *Pediatrics* 2007;119(2):247-257.
12. Dwulit AD, Rzymiski P. Prevalence, patterns and self-perceived effects of pornography consumption in polish university students: A cross-sectional study. *Int J Environ Res Public Health*. 2019;16(10):1861. doi: 10.3390/ijerph16101861.
13. Cooper A, Delmonico D, Griffin-Shelley E, Mathy R. Online sexual activity: An examination of potentially problematic behaviors. *Sexual Addiction & Compulsivity* 2004;11:129-143.
14. Voros F. The invention of addiction to pornography. *Sexologies* 2009;18:243-246. doi: 10.1016/j.sexol.2009.09.007
15. Razi NIM, Rahman AWA, Kamaruddin N. Neurophysiological analysis of porn addiction to learning disabilities, in: *Proc. Int. Conf. Inf. Commun. Technol. Muslim World 2018, ICT4M 2018*, 2018, pp. 272-277. doi: 10.1109/ICT4M.2018.00057
16. Kamaruddin N, Razi NIM, Rahman AWA. Correlation of learning disabilities to porn addiction based on EEG. *Bulletin of Electrical Engineering and Informatics*. 2021;10(1):148-155.
17. Sitarz RA, Rogers M, Jackson E, Bentley L. Analysis of Internet Addiction Among Child Pornography Users, 2011, CERIAS '11: Proceedings of the 12th Annual Information Security Symposium, West Lafayette Indiana, April 5 - 6, 2011. <https://www.cerias.purdue.edu/assets/symposium/2011-posters/C96-BA3.pdf>
18. Hughes B. "Sexual addiction": diagnosis and treatment in clinical practice. *BMC Proc*. 2012;6:P33. doi: 10.1186/1753-6561-6-s4-p33.
19. Kang X, Handayani DOD, Chong PP, Acharya UR. Profiling of pornography addiction among children using EEG signals: A systematic literature review. *Comput Biol Med*. 2020;125:103970. doi: 10.1016/j.combiomed.2020.103970.
20. Yu H, Zhao X, Li N, Wang M, Zhou P. Effect of excessive Internet use on the time—Frequency characteristic of EEG. *Prog. Nat. Sci*. 2009;19:1383-1387.
21. Lee J, Hwang JY, Park SM, Jung HY, Choi S-W, Kim DJ, Lee J-Y, Choi J-S. Differential resting-state EEG patterns associated with comorbid depression in Internet addiction. *Prog. Neuropsychopharmacol. Biol. Psychiatry* 2014;50:21-26.
22. Love T, Laier C, Brand M, Hatch L, Hajela R. Neuroscience of Internet Pornography Addiction: A Review and Update. *Behavioral Sciences*. 2015;5(3):388-433. <https://doi.org/10.3390/bs5030388>
23. Voon V, Mole TB, Banca P, Porter L, Morris L, Mitchell S, Lapa TR, Karr J, Harrison NA, Potenza MN, Irvine M. Neural correlates of sexual cue reactivity in individuals with and without

- compulsive sexual behaviours. PLoS One. 2014;9(7):e102419. doi: 10.1371/journal.pone.0102419.
24. Prause N, Steele VR, Staley C, Sabatinelli D, Hajcak G. Modulation of late positive potentials by sexual images in problem users and controls inconsistent with "porn addiction". *Biol Psychol*. 2015;109:192-199. doi:10.1016/j.biopsycho.2015.06.005
  25. Kamaruddin N, Rahman AWA, Handiyani D. Pornography Addiction Detection based on Neurophysiological Computational Approach. *Indonesian Journal of Electrical Engineering and Computer Science*. 2018;10(1):138-145. doi: 10.11591/ijeecs.v10.i1.pp138-145
  26. Kamaruddin N, Wahab A, Rozaidi Y. Neuro-Physiological porn addiction detection using machine learning approach. *Indones. J. Electr. Eng. Comput. Sci* 2019;16(2):964-971.
  27. Xiaoxi K, Handayani DOD, Kit MH. Machine Learning Classification Model for Identifying Pornography Addiction Among Children. 2021 IEEE 7th International Conference on Computing, Engineering and Design (ICCED), 2021, pp. 1-6. doi: 10.1109/ICCED53389.2021.9664849.
  28. Xiaoxi K, Handayani DOD, Wahab ABAR, Agastya IMA. Electroencephalogram (EEG) dataset with porn addiction and healthy teenagers under rest and executive function task, Mendeley Data, V5, 2021b. <https://data.mendeley.com/datasets/4r8hp2hmb4/5>. doi: 10.17632/4r8hp2hmb4.5 [accessed June 20, 2021]
  29. Xiaoxi K, Agastya IMA, Handayani DOD, Kit MH, Wahab ABAR. Electroencephalogram (EEG) dataset with porn addiction and healthy teenagers under rest and executive function task. *Data in Brief* 2021;39:107467. doi:10.1016/j.dib.2021.107467
  30. Associates T. The youth pornography addiction screening tool (YPAST). 2013. <http://www.mendingthearmor.com/lds-program-for-pornography-addiction/2013/3/10/youth-pornography-addiction-screening-tool>. *Youth Pornogr. Addict. Cent.* [accessed July 30, 2021]
  31. Mardhatillah A, Buah Hati YKd. Youth pornography exposure: addiction screening test and treatment recommendation. *Int. J. Sci. Res. Publ.* 2017;7(8):10-14.
  32. Bradley MM, Lang PJ. The international affective picture system (IAPS) in the study of emotion and attention, in: *Handbook of Emotion Elicitation and Assessment*, Oxford University Press, 2007, pp. 29–46.
  33. Soroush MZ, Maghooli K, Setarehdan SK, Motie Nasrabadi A. Emotion recognition using EEG phase space dynamics and Poincare intersections, *Biomed. Signal Process. Control* 2020;59:101918.
  34. Moridani MK, Setarehdan SK, Motie Nasrabadi A, Hajinasrollah E. A novel approach to mortality prediction of ICU cardiovascular patient based on fuzzy logic method. *Biomed. Signal Process. Control* 2018;45:160-173.
  35. Akbari H, Ghofrani S, Zakalvand P, Sadiq MT. Schizophrenia recognition based on the phase space dynamic of EEG signals and graphical features. *Biomedical Signal Processing and Control* 2021;69:102917.
  36. Gaur P, Pachori RB, Wang H, Prasad G. A multi-class EEG-based BCI classification using multivariate empirical mode decomposition based filtering and Riemannian geometry. *Expert Syst. Appl.* 2018;95:201-211.
  37. Goshvarpour A, Goshvarpour A. Poincare Indices for Analyzing Meditative Heart Rate Signals. *Biomedical Journal* 2015;38(3):229-234.
  38. Miyake A, Friedman NP, Emerson MJ, Witzki AH, Howerter A, Wager TD. The unity and diversity of executive functions and their contributions to complex “frontal lobe” tasks: A latent variable analysis. *Cognit. Psychol.* 2000;41:49-100.
  39. Stuss DT, Alexander MP. Executive functions and the frontal lobes: A conceptual view. *Psychol. Res.* 2000;63:289-298.
  40. Jurado MB, Rosselli M. The elusive nature of executive functions: A review of our current understanding. *Neuropsychol. Rev.* 2007;17:213-233.